Developmental Biology **236,** 421–435 (2001)
doi:10.1006/dbio.2001.0346, available online at http://www.idealibrary.com on IDEAL®

Limb Development in the Absence of Sonic Hedgehog Function

Chin Chiang,*,[1] Ying Litingtung,* Matthew P. Harris,† B. Kay Simandl,† Yina Li,* Philip A. Beachy,‡ and John F. Fallon†,[1]

**Department of Cell Biology, Vanderbilt University Medical Center, 1161 21st Avenue South, Nashville, Tennessee 37232; †Department of Anatomy, University of Wisconsin, 1300 University Avenue, Madison, Wisconsin 53706; and ‡Department of Molecular Biology and Genetics, Johns Hopkins University School of Medicine, Baltimore, Maryland 21205*

The secreted protein encoded by the *Sonic hedgehog* (*Shh*) gene is localized to the posterior margin of vertebrate limb buds and is thought to be a key signal in establishing anterior–posterior limb polarity. In the *Shh*$^{-/-}$ mutant mouse, the development of many embryonic structures, including the limb, is severely compromised. In this study, we report the analysis of *Shh*$^{-/-}$ mutant limbs in detail. Each mutant embryo has four limbs with recognizable humerus/femur bones that have anterior–posterior polarity. Distal to the elbow/knee joints, skeletal elements representing the zeugopod form but lack identifiable anterior–posterior polarity. Therefore, *Shh* specifically becomes necessary for normal limb development at or just distal to the stylopod/zeugopod junction (elbow/knee joints) during mouse limb development. The forelimb autopod is represented by a single distal cartilage element, while the hindlimb autopod is invariably composed of a single digit with well-formed interphalangeal joints and a dorsal nail bed at the terminal phalanx. Analysis of *GDF5* and *Hoxd11–13* expression in the hindlimb autopod suggests that the forming digit has a digit-one identity. This finding is corroborated by the formation of only two phalangeal elements which are unique to digit one on the foot. The apical ectodermal ridge (AER) is induced in the *Shh*$^{-/-}$ mutant buds with relatively normal morphology. We report that the architecture of the *Shh*$^{-/-}$ AER is gradually disrupted over developmental time in parallel with a reduction of *Fgf8* expression in the ridge. Concomitantly, abnormal cell death in the *Shh*$^{-/-}$ limb bud occurs in the anterior mesenchyme of both fore- and hindlimb. It is notable that the AER changes and mesodermal cell death occur earlier in the *Shh*$^{-/-}$ forelimb than the hindlimb bud. This provides an explanation for the hindlimb-specific competence to form autopodial structures in the mutant. Finally, unlike the wild-type mouse limb bud, the *Shh*$^{-/-}$ mutant posterior limb bud mesoderm does not cause digit duplications when grafted to the anterior border of chick limb buds, and therefore lacks polarizing activity. We propose that a prepattern exists in the limb field for the three axes of the emerging limb bud as well as specific limb skeletal elements. According to this model, the limb bud signaling centers, including the zone of polarizing activity (ZPA) acting through *Shh*, are required to elaborate upon the axial information provided by the native limb field prepattern.

Key Words: **Sonic Hedgehog function; Shh; limb development; limb patterning; zone of polarizing activity; ZPA; stylopod; zeugopod; autopod; limb field.**

INTRODUCTION

Limb pattern formation has been defined recently in terms of three signaling centers that control the three limb axes through specific signaling molecules and their downstream targets (reviewed in Ng *et al.*, 1999; Schaller *et al.*, 2001). The dorsal–ventral limb axis is controlled by the dorsal and ventral limb bud ectoderm through expression of *Wnt7a* and *En-1*, respectively (reviewed in Zeller and Duboule, 1997); proximal–distal axis elongation is controlled by fibroblast growth factor family members (FGFs) synthesized by the apical ectodermal ridge (AER) (reviewed

[1] To whom correspondence should be addressed. Fax: 615-343-4539. E-mail: chin.chiang@mcmail.vanderbilt.edu or jffallon@facstaff.wisc.edu.

0012-1606/01 $35.00

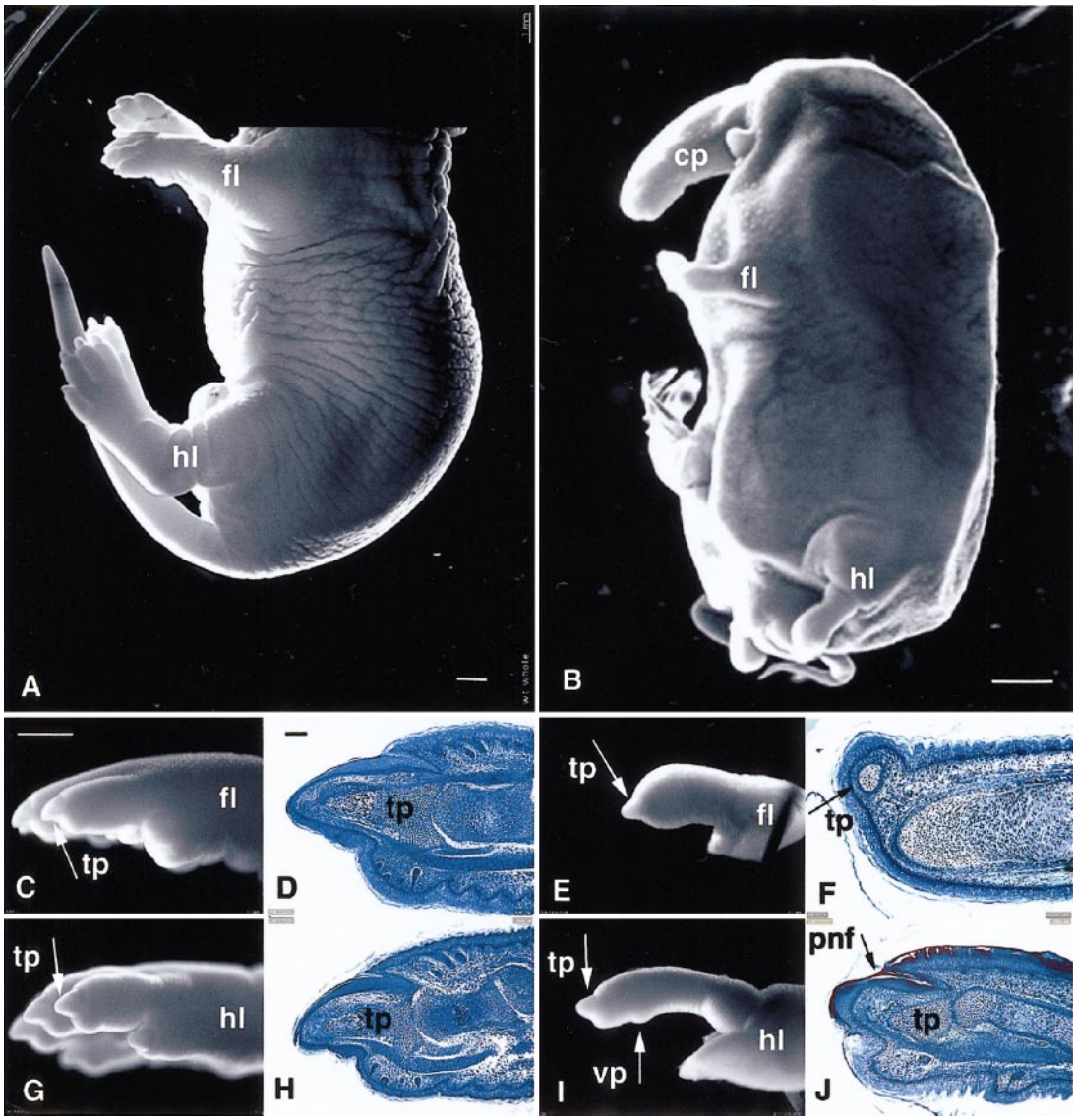

FIG. 1. 18.5-dpc wild-type and *Shh* $^{-/-}$ mutant whole body and digital surface anatomy and histology [compare A, wild-type mouse (head not shown), with B, *Shh* $^{-/-}$ mouse]. Note that the wild-type embryo is considerably larger than the mutant embryo (compare scale bar); fl, forelimb; hl, hindlimb; cp, cephalic proboscis. Comparison of (C), wild-type forelimb autopod, with (E), *Shh*$^{-/-}$ forelimb autopod, shows that both wild-type and mutant digits end with a terminal phalanx (tp). Histological data show that in (D), the wild-type forelimb digit terminal phalanx forms a joint with the next most proximal phalanx and there are the expected dorsal–ventral asymmetries (top/bottom, respectively). (F) The *Shh*$^{-/-}$ mutant forelimb autopod is represented by a single skeletal element that does not form a jointed relationship with the next most proximal element. The "terminal phalanx" (tp) of the mutant forelimb is the sole representation of the forelimb autopod. Notice, there are dorsal and ventral asymmetries in the mutant epidermis, as shown by the presence of incipient dorsal hair follicles. The *Shh*$^{-/-}$ hindlimb autopod (I) and wild-type control (G) both end in a terminal phalanx (tp) and show dorsal–ventral asymmetries, which include ventral (volar) protrusions (vp). Comparison of histological detail shows that both the wild-type hindlimb (H) and mutant (J) terminal phalanges are comparable including the proximal nail fold (pnf) and joints. Note the presence of ventral pads and ventral glands in the mutant. For all surface anatomy, the scale bar equals 1 mm; if not shown, the scale of the pictures is the same as in (C). In the histological sections, the scale bar in (D) is equal to 0.1 mm and is the same for each section shown.

in Martin, 1998); and the anterior–posterior limb axis is controlled by Sonic hedgehog (*Shh*) synthesized by a small group of mesodermal cells along the postaxial limb bud border called the zone of polarizing activity (ZPA). When grafted beneath the preaxial AER, either ZPA cells or the recombinant amino-terminal product of *Shh* (SHH-N)

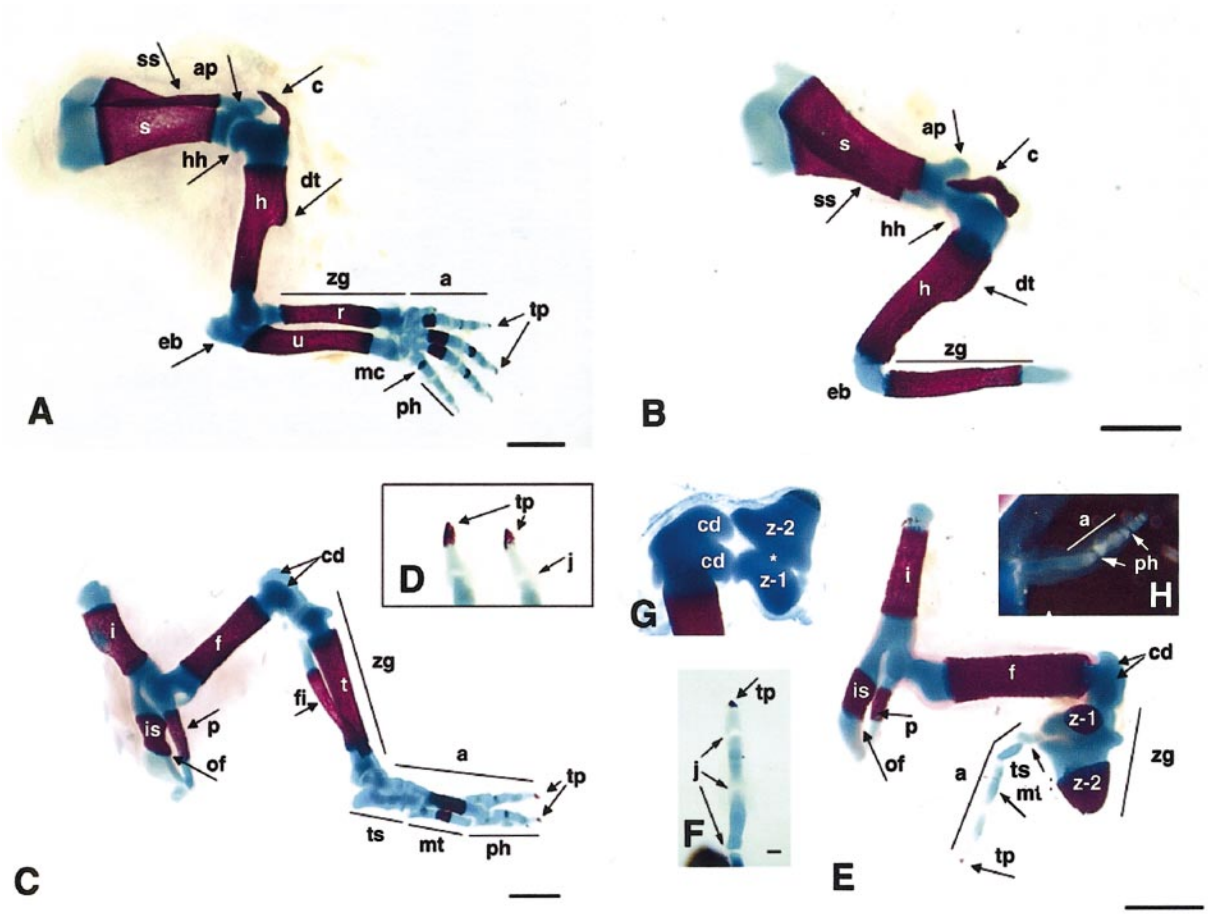

FIG. 2. Limb skeletal development at 17.5 dpc in wild-type and *Shh*$^{-/-}$ mice stained with alizarin red and Alcian blue. Compare wild-type forelimb skeleton (A) with *Shh*$^{-/-}$ mutant forelimb skeleton (B). Both show comparable shoulder girdle elements (s, c) and humerus (h). At the stylopod/zeugopod junction, the mutant phenotype can be seen. At the mutant elbow joint (eb), the humerus (h) is connected by solid cartilage (blue) to a single zeugopod element (zg) that is ossified (red) along its length and ends in a cartilaginous extension. The distal phalanx shown in Figs. 1E and 1F was always lost when the skin was removed for skeletal staining. Compare wild-type hindlimb skeleton (C) with *Shh*$^{-/-}$ mutant hindlimb skeleton (E). Both show comparable pelvic girdle (i, is, p) and femur (f) development. The mutant knee joint (G) is recognizable in that the femoral condyles (cd) show a relationship with two cartilaginous zeugopod elements (Z-1, Z-2) that invariably are fused (*) in the midline. Distal to Z-1 and Z-2 and not connected to them is a series of cartilaginous rods separated by joints (j); compare (j) in (F) with (D). The most proximal rod, representing the tarsal bone (ts), emerges from between Z-1 and Z-2. It is thought that the next short cartilage element is a fractured component of the tarsus followed by two longer elements (E, F). A different mutant hindlimb specimen (H) shows at higher magnification the metatarsus and the presence of two phalanges (ph) distal to it. At the end of the mutant autopod element (a) is an arrowhead-shaped ossification center of the terminal phalanx (tp) that stained with alizarin red and is slightly smaller but comparable to the ossification center of the wild-type terminal phalanx (compare tp in F and D). Abbreviations: s, scapula; ss, spine of scapula; ap, cartilage of proximal acromion; c, clavicle; hh, head of humerus; h, humerus; dt, deltoid tuberosity; eb, elbow joint; zg, zeugopod; r, radius; u, ulna; a, autopod; mc, metacarpals; ph, phalanges; tp, ossification center of terminal phalanx; I, iliac bone; is, ischial bone; p, pubic bone; of, obturator foramen; f, femur; cd, femoral condyles; fi, fibula; t, tibia; z, zeugopod; Z-1, smaller *Shh*$^{-/-}$ zeugopod element; Z-2, larger *Shh*$^{-/-}$ zeugopod element; ts, tarsal bones; mt, metatarsal bones; j, digital joint articulations. All bars equal 1 mm, except (F), which equals 0.1 mm.

(Lopez-Martinez *et al.*, 1995; Yang *et al.*, 1997) will induce mirror-image duplications in host wings (reviewed in Pearse and Tabin, 1998). This ability to induce extra digits to form is called polarizing activity (summarized in Tanaka *et al.*, 2000) and SHH-N is sufficient to mediate this activity. The three signaling centers appear to be interdependent for both their maintenance and function (reviewed in Johnson and Tabin, 1997).

Presently it is thought that signaling by *Shh* occurs through the transmembrane proteins patched (*Ptch*) and smoothened (*Smo*). In the absence of *Shh*, *Ptch* inhibits *Smo* activity, whereas *Shh* binding to *Ptch* relieves this inhibi-

tion. *Smo* then transduces the signal causing changes in activity of the *Gli* gene products (vertebrate homologues of the *Drosophila cubitus interuptus* gene) and mediates downstream gene transcription (reviewed in Pearse and Tabin, 1998). *Shh* signaling results in the upregulation of *Ptch* and *Gli1* expression in ZPA cells. This is followed by a rapid increase in levels of bone morphogenetic protein 2 (*Bmp2)* transcripts, and the 5′ *Hoxd* gene cluster (specifically, *Hoxd11*, *d12*, and *d13*) in the mesoderm adjacent to the ZPA (Nelson *et al.,* 1996). Zúñiga *et al.* (1999) have shown that *Shh* signaling regulates the expression of *Formin* and the BMP antagonist *Gremlin* in the limb bud mesoderm adjacent to the ZPA and under the AER. These authors propose that the function of *Formin* is to mediate the expression of *Gremlin*, which carries out the interaction between the ZPA and the AER. While a feedback loop has been hypothesized between continued *Fgf4* expression in the AER and *Shh* expression by ZPA cells (Pearse and Tabin, 1998), recent evidence from conditional knockouts of *Fgf4* in the mouse AER indicates that *Shh* expression and normal limb development are not dependent on AER *Fgf4* function (Moon *et al.,* 2000; Sun *et al.,* 2000).

A variety of experiments have been carried out in chick and mouse embryos to attempt to determine what effect the loss of the ZPA or *Shh* expression would have on limb development. Studies using chemical treatment or microsurgical manipulation (e.g., Bell *et al.,* 1999; Pagan *et al.,* 1996; Stratford *et al.,* 1996) were not as informative as hoped because of potential nonspecific effects of the chemical treatment used and because microsurgical techniques may damage the AER and/or reduce the amount of mesoderm below a critical mass required for normal development. However, targeted disruption of the *Shh* gene also has been reported (Chiang *et al.,* 1996); this provides the definitive opportunity to study the role of *Shh* in limb development without the caveats associated with microsurgery or chemical treatment. It was reported that $Shh^{-/-}$ embryos show dramatic and specific developmental defects that correlate with the spatial and temporal expression of *Shh* and its proposed role in signaling networks. In the limbs, distal defects were noted. Here, we report in detail on the development of $Shh^{-/-}$ mouse limbs.

MATERIALS AND METHODS

Animals

The generation and identification of *Shh* homozygous mutant mice and embryos are as described in Chiang *et al.* (1996). White Leghorn chick embryos of the Babcock strain were maintained at the University of Wisconsin. Chick embryos were staged according to the Hamburger and Hamilton series (Hamburger and Hamilton, 1951).

Skeletal Staining and Histological Sections

The skin and viscera of 18.5-dpc embryos were removed and the embryos fixed in 95% ethanol. Cartilage and bone were stained with Alcian blue and alizarin red as described (Kochhar, 1973).

For autopod histology, 18.5-dpc wild-type and $Shh^{-/-}$ fore- and hindlimb digits were fixed in Bouin's fixative, embedded in JB-4 medium, and sectioned at 4-μm thickness with a JB4 Sorvall microtome using glass knives. Sections mounted on glass slides were stained with methylene blue, azure II in 1.0% aqueous borax, cover slipped, and viewed. Early limb buds from 10.5-, 11.5-, and 12.5-dpc wild-type and $Shh^{-/-}$ mutant mice were fixed and processed in similar manner. Sections of 1-μm thickness were made in a transverse cross section to the AER in anterior, mid, and posterior locations to permit visualization of anterior–posterior changes in AER structure.

BrdU and TUNEL Analysis

Forelimbs and hindlimbs of 10.5- and 11.5-dpc embryos were dissected with attached lateral tissue, which serves as a reference for anterior–posterior orientation of the limb. Limbs were dehydrated and embedded in paraffin. Serial sections, parallel to the proximal–distal axis of the limb, were collected onto glass slides. TUNEL and BrdU labelings were performed as previously described (Litingtung *et al.,* 1998). Apoptotic cells were visualized by TUNEL according to the manufacturer's specification (Intergen, New York).

Whole-Mount In Situ Hybridization

Embryos at 10.5 dpc were dissected from their extraembryonic membranes and fixed in 4% paraformaldehyde in phosphate-buffered saline. Whole-mount *in situ* hybridization was performed essentially as previously described (Henrique *et al.,* 1995). The following probes were used: *BMP2* (B. Hogan); *Bmp4* and *Gdf5* (S. Lee); *Fgf4* and *Fgf8* (G. Martin); *Msx-2* (R. Maxson); *Ptch1* (M. Scott); *Ptch2*, *Gli1*, and *Gli3* (C-c. Hui); *Hoxd11*, *Hoxd12*, and *Hoxd13* (D. Duboule); *En-1* (A. Joyner); *Wnt7A* (A. McMahon); *Formin* (P. Leder); and *Msx1* (B. Robert).

Zone of Polarizing Activity Grafts

Mesoderm tissue was dissected from the posterior border of 10.5-dpc $Shh^{-/-}$ limb buds. A small piece of mesoderm tissue was then grafted under the anterior apical ridge of stage-18–20 chick host limb buds. Host embryos were allowed to develop to 10 days, fixed in 10% formalin, stained with Victoria blue, and cleared in methyl salicylate to visualize the cartilage patterns (Ros *et al.,* 2000).

RESULTS

All vertebrate limbs have a similar structure composed of three proximal-to-distal segments: the stylopod (humerus or femur), the zeugopod (radius/ulna or tibia/fibula), and the autopod (wrist/hand or ankle/foot) (Stocum, 1995). While the proximal two limb segments exhibit relatively little variation across tetrapods, the autopod is highly variable.

Shh$^{-/-}$ *Embryo Limb Morphology*

External morphology, terminal phalanx, and dorsal–ventral polarity. Fifteen *Shh*$^{-/-}$ mutant embryos were compared with age-matched wild-type siblings (representative specimens shown in Figs. 1A and 1B). The mutant embryos were always smaller than wild-type littermates but each had four short appendages at the correct anatomical locations on the body. In every limb, at the gross level of observation, there appeared to be a single terminal phalanx that was similar to that of the wild-type digits (compare Figs. 1C and 1G with Figs. 1E and 1I).

The mutant forelimb terminal phalanx appeared conical when compared with the more claw-like wild-type forelimb structure (compare Fig. 1C with Fig. 1E). Histological sections (compare Fig. 1D with Fig. 1F) showed that, in fact, the mutant forelimb terminated in a single cartilaginous carpal-like element that did not form a joint with the next most proximal element and no nail bed was present. The distal element did not form a connection with the proximal element, as it could be separated when the skin of the forelimb was removed during preparation for skeletal staining. There were no external distinguishing dorsal–ventral characteristics visible on the mutant forelimb, however, in histological sections, as reported previously (Chiang *et al.*, 1999; St-Jacques *et al.*, 1998), there were incipient hair follicles marking the dorsal skin that were absent on the ventral surface.

The *Shh*$^{-/-}$ mutant hindlimb terminal phalanx was similar to the corresponding wild-type structure (compare Fig. 1G with Fig. 1I). There appeared to be a ventral curvature to the digit and at least one ventral pad (VP; Fig. 1I) was always present; some specimens had two or three ventral pads. Histological sections (compare Fig. 1H with Fig. 1J) confirmed that there was a jointed terminal phalanx, with a proximal nail fold, beginning nail growth, and other obvious dorsal–ventral characters including incipient dorsal hair follicles, dermal cell concentrations embodying the ventral pads, associated gland structures, and ventral tendons. A recent publication by Kraus *et al.* (2001) describes similar anatomy of the terminal element of the fore- and hindlimb of the *Shh*$^{-/-}$ mutant mouse. Additionally, the authors show evidence that the dorsal epidermis of the hindlimb terminal phalanx expresses keratins specific to nail and hair keratinocytes. This complements the histological descriptions presented here identifying the terminal dorsal structure as a nail.

Forelimb skeletal anatomy. The limb skeletal patterns of seven mutant and wild-type 17.5–18.5-dpc embryos were analyzed (compare Figs. 2A and 2C with Figs. 2B and 2E). The pectoral girdle of the *Shh*$^{-/-}$ mutant appeared to be normally formed. An identifiable scapula with coracoid process (not shown) and clavicle was present in all mutant specimens. The proximal part of the stylopod was identifiable as a humerus with a deltoid tuberosity and a humeral head that articulated with the scapula. No mutant specimen had a joint at the elbow; however, each forelimb showed a bend where the elbow is expected. The region of the bend was composed of cartilage while the single elements proximal and distal to the bend were ossified.

Hindlimb skeletal anatomy. The *Shh*$^{-/-}$ mutant pelvic girdle appeared to be normally formed (compare Fig. 2C with Fig. 2E) with an ossifying os, pubis, and ischium. The mutant femur appeared normal with well-defined head, neck, shaft, and two condyles (cd). Two distinct but incomplete elements represented the *Shh*$^{-/-}$ mutant zeugopod, one larger (Z-2) than the other (Z-1). The proximal ends of these elements were cartilaginous and formed a knee joint with femoral condyles. This was best seen in a ventral view (Fig. 2G). The middle of the two zeugopod elements invariably showed a cartilage fusion (asterisk, Fig. 2G) linking the two; the distal part of the larger element (Z-2) had begun ossification. In the context of the knee joint, these two truncated elements appear to represent the tibia (Z-2) and fibula (Z-1) bones. A single digit that consisted of a tarsal bone (t; Fig. 2E), the metatarsal (mt), and two phalanges represented the autopod of the leg (Figs. 2E and 2H). The proximal autopod elements had not begun ossification. However, the mutant terminal phalanx invariably showed ossification (compare Figs. 2C and 2D with Figs. 2E and 2F) that was morphologically similar to the wild-type terminal phalanx.

Molecular Analysis of Digit Formation

To analyze the character of the autopod structures further, we took two approaches. The first of these was to compare the expression of *Gdf5*, a bone morphogenetic protein family member whose expression occurs in the interphalangeal cells of the forming digital joints (Storm and Kingsley, 1996). In outgrowth of the mutant embryo forelimb, there was no detectable expression of *Gdf5* at 14.5 dpc, at a stage when there is robust expression in the wild-type presumptive joints (compare Figs. 3A and 3B). This is consistent with our observations of the 18.5-dpc histology in which the terminal element of forelimb cartilage did not appear to have a typical jointed relationship with the proximal limb skeleton. The mutant hindlimb autopod interphalangeal cells, however, did express *Gdf5* at 14.5 dpc (compare Figs. 3C and 3D). Interestingly, *Gdf5* is only expressed in two domains in the forming digit, similar to wild-type digit one. The *Gdf5* expression data provide a molecular foundation for the interpretation that the mutant hindlimb forms a digit and suggest that the forming digit represents digit one. We further demonstrated that *Msx1* expression, which marks the nail bed cells on the dorsum of the terminal phalanx (Reginelli *et al.*, 1995), was expressed similarly in normal and mutant hindlimb digits (Figs. 3G and 3H); *Msx1* was undetectable in the mutant forelimb digit (Figs. 3E and 3F). We conclude that stylopod, zeugopod, and autopod elements form in *Shh*$^{-/-}$ limbs.

To further explore the possible digit-one identity of the hindlimb digit suggested by *Gdf5* results, we extended our analysis of digit formation by looking at the expression of

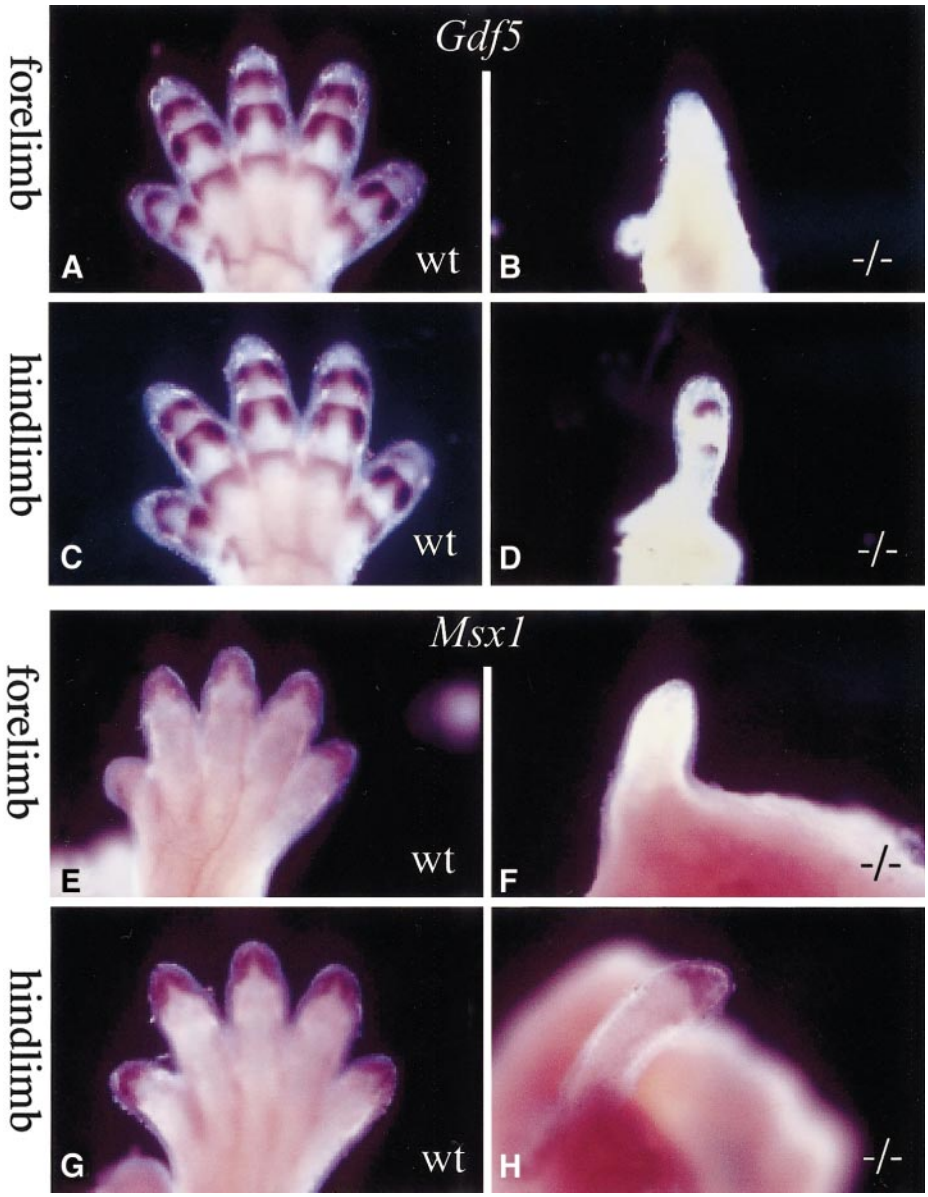

FIG. 3. Molecular analysis of autopod patterning*: Gdf5* and *Msx1*. Expression of *Gdf5* in the forming joints of forelimbs (A, B) and hindlimbs (C, D) in wild-type (A, C) and $Shh^{-/-}$ mutant (B, D) limbs at 15.5 dpc. Expression of Msx1 in the nail beds of forelimbs (E, F) and hindlimbs (G, H) in wild-type (E, G) and $Shh^{-/-}$ mutant (F, H) at 17.5 dpc. Note the patterned expression of *Gdf5* and *Msx1* in $Shh^{-/-}$ hindlimbs.

Hoxd11–13 in the forming autopodial structures of wild-type and mutant limbs. *Hoxd11–13* are expressed in a *Shh*-dependent fashion in the forming autopod of chicken and mice (Nelson *et al.*, 1996; Shubin *et al.*, 1997) and are thought to impart a dose-dependent mechanism for proliferation and growth of forming phalangeal structures (Zákány and Duboule, 1999; Zákány *et al.*, 1997). Analysis of *Hoxd11* and *-d12* expression in 11.5- and 12.5-dpc wild-type fore- and hindlimbs show the characteristic phase II *Hoxd gene* expression along the posterior presumptive zeugopod (Figs. 4A, 4E, 4I and 4M) and initial autopod expression characteristic of phase III *Hoxd* gene (Nelson *et al.*, 1996). A comparison with mutant limbs at this stage demonstrates an absence of *Hoxd12* and *-d13* phase II expression in both mutant fore- and hindlimbs (Figs. 4J, 4N, 4R, and 4V). *Hoxd11* expression, however, is maintained at reduced levels in both fore- and hindlimbs. The absence of *Shh*-dependent *Hoxd12* and *d13* phase II expression correlates

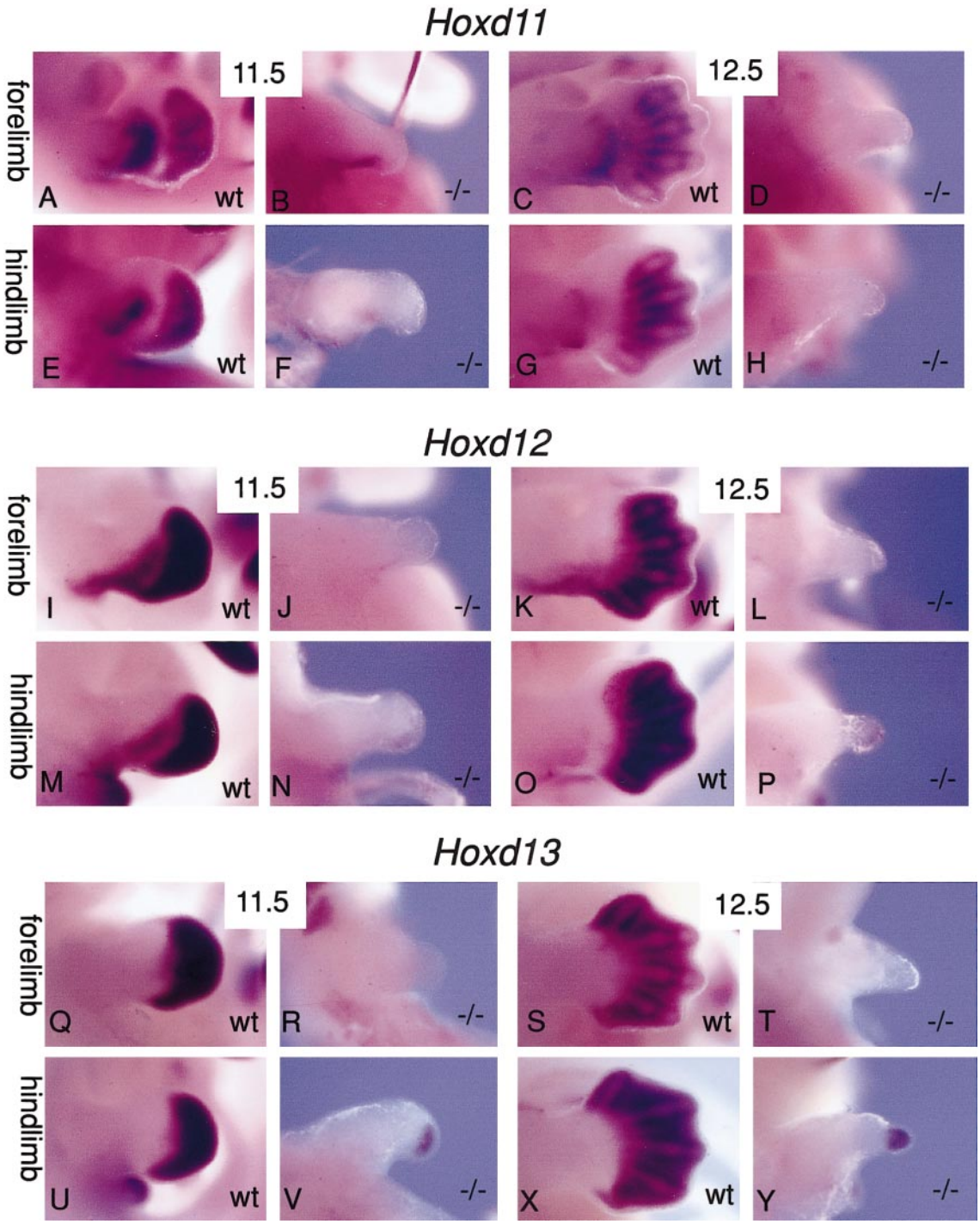

FIG. 4. Molecular analysis of autopod patterning: *Hoxd11–13*. Autopod expression of *Hoxd11–13* in *Shh*$^{-/-}$ limbs. Whole-mount *in situ* hybridization of wild-type and *Shh*$^{-/-}$ mutant limbs with probes against *Hoxd11* (A–H), *Hoxd12* (I–P), and *Hoxd13* (Q–Y) at 11.5 and 12.5 dpc. *Hoxd11–13* genes are differentially expressed in the autopod of both wild-type and mutant limbs. The expression of *Hoxd11* and -*d12* genes does not extend to the most anterior digit one of wild-type limbs (A, E, C, G and I, M, K, O) while *Hoxd13* expression is extended across the whole autopod (Q, U, S, X). Mutant forelimbs show no *Hoxd11–13* expression in the autopod (B, D, J, L, R, and T). In contrast, mutant hindlimbs show extensive *Hoxd13* expression throughout the autopod (V, Y) and lack detectable *Hoxd11* and have reduced *Hoxd12* (F, H, N, P).

with the anatomical loss of anterior–posterior polarization of the zeugopodial structures of both mutant limbs (noted above). The expression of *Hoxd13* in the forming autopod of 12.5-dpc wild-type limbs encompasses the digit-one primordia (Figs. 4S and 4X), whereas *Hoxd11* and -*d12* expression is restricted posteriorly to encompass digits two through five (Figs. 4C, 4G, 4K, and 4O). In the mutant, *Hoxd13* is expressed throughout the entire hindlimb autopod, but not in the mutant forelimb. In contrast, only distal low levels of *Hoxd12* are seen in the mutant hindlimb and *Hoxd11* is not detected. These data complement the *Gdf5* analysis of joint formation and support the conclusion that the hindlimb digit is specified and represents digit one. The mutant forelimb shows no autopodial expression of *Hox d11–13* consistent with its failure to realize distal phalangeal fates.

Shh$^{-/-}$ Limb Buds Do Not Have Polarizing Activity

Polarizing activity can occur in the absence of *Shh* expression. For example, tissues expressing Indian hedgehog (*Ihh*) (Yang *et al.*, 1998), as in the *Doublefoot* mutant mouse limb bud, will cause mirror-image duplications when grafted to a chick embryo host wing bud anterior borders (Hayes *et al.*, 1998). We therefore examined whether the *Shh*$^{-/-}$ mutant mesoderm had polarizing activity when grafted to a host chick limb bud. In controls, wild-type mouse ZPA grafted to the chick induced mirror-image duplications in 9 of 20 cases (45%); grafts of mouse ZPA tissue are less efficient in producing mirror-image duplications than chick ZPA grafts to chick wing buds (Fallon and Crosby, 1975; Tanaka *et al.*, 2000). The digit sequence in response to wild-type mouse ZPA grafts in increasing order of complexity included four cases of 2234, two cases of 32234, one case of 2324, and two cases of 432234 (see Fig. 5A). In the *Shh*$^{-/-}$ posterior border grafts, 14 grafts were made and all (100%) showed a normal digit pattern of 234 at day 10 (see Fig. 5B). These data indicate that the *Shh*$^{-/-}$ limb buds do not have polarizing activity and that the zeugopod and autopod elements that form in the *Shh*$^{-/-}$ mutant do so without the input of polarizing activity.

Polarized Gene Expression in the Limb Bud Does Not Require Shh Function

Shh activity in the posterior margin of the limb bud has been implicated in the establishment of polarized expression of *5′Hoxd* genes in the mesoderm and *Fgf4* in the AER. Ectopic expression of *Shh* protein in the anterior margins of chick limb buds induces ectopic mesoderm expression of *5′Hoxd* and AER expression of *Fgf4* (Pearse and Tabin, 1998). Interestingly, the limb buds of the chick *limbless* mutant do not express *Shh*, but express *Hoxd11–13* in an asymmetric pattern (Grieshammer *et al.*, 1996; Noramly *et al.*, 1996; Ros *et al.*, 1996a). We therefore examined expression of genes implicated in *Shh* signaling to determine the effect of the *Shh* mutation on the molecular differentiation in the early limb bud. Several AER markers, including *Fgf8* (Figs. 6C and 6D), *Bmp4* (Figs. 6E and 6F), and *Msx2* (data not shown), are expressed in 10.5-dpc *Shh*$^{-/-}$ mutant limbs, although *Fgf8* expression becomes reduced as development proceeds (see below). *Fgf4* expression, which is restricted to the posterior two-thirds of the AER, is also present in the mutant (Figs. 6A and 6B; see also Zúñiga *et al.*, 1999), although its expression is detectable only in the hindlimb at 10.5 dpc in our mutant line.

Some of the genes normally expressed in the limb mesoderm were also present in the mutant, but generally did not have a normal distribution or normal levels of expression, whereas the expression of other genes was absent. *Bmp4* is expressed in preaxial and postaxial *Shh*$^{-/-}$ mutant limbs and shows a distribution comparable to that of wild type, but at reduced levels (Figs. 6E and 6F). *Bmp2* expression is detectable in the mutant forelimb postaxial mesoderm, but at substantially reduced levels (Figs. 6G and 6H). In addition, the AER expression of *Bmp2* is not detected in *Shh*$^{-/-}$ mutant limbs (Figs. 6G and 6H). Similar to *limbless* limb buds, *Hoxd11* and *Hoxd12* are present in the postaxial mesoderm (Figs. 6I and 6J; and data not shown), but the extent of expression is limited to the postaxial border mesoderm of the mutant buds. We were not able to detect *Hoxd13* in the *Shh*$^{-/-}$ mutant forelimb buds, but it was detected at reduced levels and with greatly reduced distribution in the hindlimb postaxial mesoderm (Figs. 6K and 6L). Along with the *5′Hoxd* genes, the proposed downstream targets of *Shh* signaling showed modified expression patterns. *Ptch1* (Figs. 6M and 6N), *Ptch2* (not shown), and *Gli1* (Figs. 6O and 6P) were not detectable in the *Shh*$^{-/-}$ buds. *Formin*, normally expressed in the posterior limb bud mesoderm (Fig. 6Q) and implicated in AER maintenance, was not expressed in *Shh*$^{-/-}$ mutant limbs (Fig. 6R). This confirms a recent report by Zúñiga *et al.* (1999). *Gli3* also shows a modified expression pattern in mutant buds in that expression was detected throughout the bud extending to the border of the postaxial mesoderm (Figs. 6S and 6T), suggesting *Shh* normally represses *Gli3* expression in the posterior mesoderm. A similar negative role of *Shh* on *Gli3* transcription has been reported in chick micromass culture (Wang *et al.*, 2000).

Dorsal–ventral polarity is controlled by the dorsal and ventral limb bud epithelia through the expression of *Wnt7a* and *En-1*, respectively. Both of these genes are expressed normally by the mutant dorsal and ventral epithelia (data not shown; see also Kraus *et al.*, 2001). This was further indicated by the incipient dorsal hair follicles on both autopod structures as well as the ventral surface protrusions and tendons of the hindlimb digit that are described above (see Figs. 1F and 1J).

Shh$^{-/-}$ Apical Ectodermal Ridge Structure and Fgf8 Expression

We next examined the interrelationship between *Shh* and AER maintenance by looking at a time course of *Fgf8*

expression in concert with histological analysis of AER structure during limb outgrowth. As described above in Figs. 6C and 6D (see also Kraus *et al.*, 2001; Sun *et al.*, 2000), *Fgf8* was present in the AER of both the fore- and hindlimb of *Shh* mutants at 10.5 dpc. We extended this analysis up to 12.5 dpc to assess the relationship of *Fgf8* expression and AER ridge structure in *Shh*$^{-/-}$ mutant limb buds. Although *Fgf8* expression was detected in mutant 11.5-dpc limbs, there was a distinct change in the height and organization of the AER when compared to control sections. This disorganization began in the AER as early as 10.5 dpc of both fore and hind mutant limb buds (Fig. 6D, and data not shown). In both the fore- and hindlimb, the reduction of *Fgf8* expression correlated temporally with the change in AER morphology (compare Figs. 7I, 7M, 7K, and 7O with Figs. 7J, 7N, 7L, and 7P). This is exemplified by the 12.5-dpc mutant forelimb where regions of reduced *Fgf8* expression in the middle bud exhibit no apparent AER structure (Figs. 7J and 7N). Sections of the posterior AER of the 12.5-dpc limb bud, showing persistent expression of *Fgf8*, maintained a stratified squamous AER morphology (Fallon and Kelley, 1977); data not shown). A comparison between fore- and hindlimb 12.5-dpc AER clearly showed that the AER was maintained longer in the mutant hindlimb and correlated with the formation of a complete digit (compare Figs. 7J and 7N, and Figs. 7L and 7P). At the same time, loss of ridge structure and signaling in the forelimb correlated with limb truncation.

Cell Death and Proliferation in Shh Mutant Limbs

In addition to the early reduction of AER structure in the mutant forelimb, we noticed a decrease in anterior expression of *Fgf8* in both fore- and hindlimb buds of the *Shh*$^{-/-}$ mutant (arrow in Figs. 7B and 7D). It was thought that both of these observations could represent changes in either cell proliferation and/or cell death in the mutant limb that may affect positioning and or maintenance of the AER and subsequently distal patterning of the limb. Therefore, we looked at the incorporation of BrdU as well as TUNEL labeling in *Shh*$^{-/-}$ and wild-type 10.5- and 11.5-dpc limb buds. Although there was a general decrease in proliferation in the mutant at 11.5 dpc (data not shown), there was not an obvious asymmetry in proliferation during these stages. However, mutant forelimb buds did show a significant increase in cell death in 10.5-dpc limb buds over either the hindlimb or wild-type limbs at comparable stages (Figs. 8A, 8B, 8E, and 8F). The TUNEL data are supported by the presence of apoptotic bodies in the 10.5-dpc mutant forelimb seen in histological sections (data not shown). By 11.5 dpc, the mutant hindlimb showed a similar increase in cell death as seen in the forelimb (Fig. 8H). Cell death in both mutant limb buds was concentrated in the anterior mesoderm, and coincided with asymmetric loss of Fgf8 expression in the mutant AER. No appreciable cell death was detected in wild-type limb buds (Figs. 8A, 8C, 8E, and 8G).

DISCUSSION

It is notable that *Shh*$^{-/-}$ mutant limbs show little variation in skeletal pattern from one embryo to another, indicating that a precise limb developmental program is replicated in all the *Shh*$^{-/-}$ mutants. Because of this, we propose that the skeletal elements present in the *Shh*$^{-/-}$ mutant limbs are specified in the limb-field mesoderm as a prepattern and subsequently are determined by the permissive action of the AER. It follows that specification of the three limb axes is initiated in the limb field in the absence of *Shh*. In this model, realization of the normal wild-type limb phenotype depends on the action of the three limb signaling centers in the context of the limb-field prepattern.

The early mutant limb buds appear morphologically normal, but the posterior border mesoderm does not express *Ptch1*, *Ptch 2*, and *Gli1*, nor does it induce extra digits in a chick limb bud bioassay for hedgehog family members. Nevertheless, *Hoxd11*, *-d12*, and *-d13* are asymmetrically expressed in the 10.5-dpc mutant postaxial limb bud mesoderm. The *Shh*$^{-/-}$ mutant limb bud mesoderm has the ability to induce and maintain an AER that permits elongation of the limb bud. The mutant AER transiently expresses *Fgf4* (Zúñiga *et al.*, 1999) and weakly expresses *Fgf9* and *-17* (Sun *et al.*, 2000). However, *Fgf8* expression appears normal in the early limb bud (Kraus *et al.*, 2001; Sun *et al.*, 2000; this report) and then declines coincident with the thinning and disruption of AER morphology. Given the apparent similarity of various Fgf activities in the limb, an integrated view of Fgf family expression will be required to understand the relationship between Fgf signaling and AER function (cf., Lewandoski *et al.*, 2000; Moon *et al.*, 2000; Moon and Capecchi, 2000; Sun *et al.*, 2000).

Morphologically, the limb defect in *Shh*$^{-/-}$ is noticeable by 11.5 dpc, where both fore- and hindlimbs have a relatively narrow and pointed appearance (cf. Fig. 7). Previous studies have suggested that *Shh* may function as a survival factor in the neural tube, lung, and head mesenchyme (Ahlgren and Bronner-Fraser, 1999; Borycki *et al.*, 1999; Litingtung *et al.*, 1998). Similarly, in the limb, the absence of *Shh* leads to an increase in cell death primarily in the anterior region of the forming limb bud. This anterior cell death is reminiscent of the extensive anterior cell death in chick limb buds following removal of posterior mesoderm including the ZPA (Todt and Fallon, 1987). Interestingly, Sanz-Ezquerro and Tickle (2000) have reported that releasing SHH-N from a bead into the chick anterior limb bud mesoderm prevents normally occurring anterior necrotic zone cell death. These observations together with the cell death in the anterior mesoderm of the *Shh*$^{-/-}$ limb buds point to a role for the ZPA and *Shh* in anterior limb bud mesoderm cell survival.

With regard to pattening of limb elements, it appears that the stylopod (humerus/femur) is completely specified, including anterior–posterior polarity, in the absence of *Shh* function. The zeugopod and autopod also develop in the absence of *Shh*, but are incomplete and lack normal

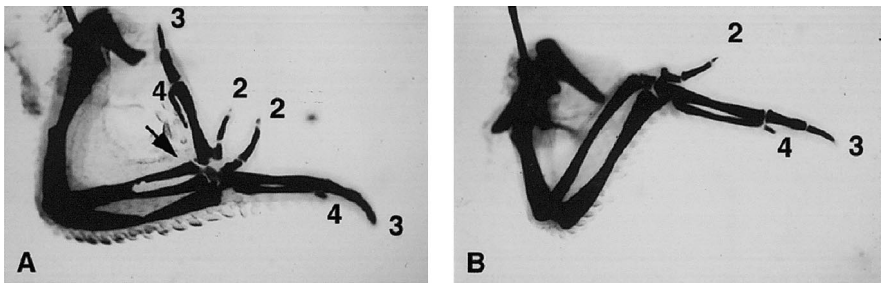

FIG. 5. Polarizing activity assay. (A) A stage-20 host chick wing bud received a sub ridge graft of wild-type mouse ZPA and formed a mirror-image duplication shown at 10 days after Victoria blue staining. The distal radius (arrow) is duplicated and the digital pattern is 4-3-2-2-3-4. (B) A normal wing that developed after $Shh^{-/-}$ postaxial border mesoderm was grafted under the host AER. The digital pattern is 2-3-4.

anterior–posterior asymmetry. It is notable that the fore- and hindlimb zeugopod elements are not comparable. The forelimb forms a single elongated zeugopodial bone without an elbow joint. In contrast, the mutant hindlimb zeugopod is composed of two short elements that form a knee joint proximally but are severely truncated distally. It is not obvious why fore- and hindlimb zeugopod morphogenesis should be so different in the absence of *Shh* function. Because the action of the AER on the subjacent mesoderm is permissive rather than instructive (Martin, 1998; Rubin and Saunders, 1972; Zwilling, 1955, 1964), a second conclusion of our studies is that the three proximal–distal limb levels, stylopod, zeugopod, and autopod, are specified in the limb field. The evidence for a limb-field prepattern adds a level of complexity for the role of *Shh* in limb development.

The ability of $Shh^{-/-}$ limbs to generate all three proximal–distal limb segments demonstrates that proximal-to-distal determination of fates is occurring in $Shh^{-/-}$ mutant limbs. The continued $Shh^{-/-}$ mutant limb bud elongation is probably due to persistent *Fgf8* expression (see Fig. 7) detected in the mutant AER. The nature of the skeletal elements of the zeugopod of the $Shh^{-/-}$ mutant limbs precludes identification as anterior (preaxial) or posterior (postaxial). However, several lines of evidence suggest that the single hindlimb digit of the $Shh^{-/-}$ mutant represents digit one of the foot. First, analysis of the *Shh* mutant hindlimbs showed that the mutant digit had only two phalanges; digit one is the only foot digit with two phalanges, in the wild-type limb. Second, *Gdf5* expression shows the presence of only two forming joints in the $Shh^{-/-}$ hindlimb digit primordium. Finally, digit-one development in the wild-type autopod is marked by *Hoxd13* expression in the digit primordium in the absence of similar expression of *Hoxd11* and *-d12*. The forming $Shh^{-/-}$ mutant hindlimb digit shows expression of *Hoxd13* throughout, but does not have detectable *Hoxd11* and reduced expression of *Hoxd12*. The comparison between the mutant and wild-type expression patterns of *Hoxd11–13* suggests that the mutant autopod has anterior specification and, specifically, digit-one fate.

Our detailed analysis revealed that $Shh^{-/-}$ limbs, relative to normal limbs, are specified along the anterior–posterior, dorsal–ventral, and proximal–distal axes through the entire stylopod and become deficient in anterior–posterior patterning distally with only proximal–distal/dorsal–ventral polarity in the zeugopod and autopod. This indicates the necessary nature of *Shh* input at or just distal to the stylopod/zeugopod transition (elbow/knee levels) during limb development. The role of *Shh* in normal limb development would be to stabilize and expand the limb-field prepattern specifying those elements not found in the $Shh^{-/-}$ mutant buds. To do this, *Shh* must stabilize and amplify asymmetric gene expression arising from the limb field [e.g., *Hoxd11*, *-d12* and *-d13*, *-dHand* (Charité *et al.*, 2000; Fernandez-Teran *et al.*, 2000); *Formin*, *Gremlin* (Zúñiga *et al.*, 1999)] and add others [e.g., *Hox11–13* paralogous genes (Nelson *et al.*, 1996)]. Together with *Shh*-dependent proliferation, the regulation of patterning genes by *Shh* would result in the expansion of the limb prepattern to the full three-dimensional limb skeleton of the zeugopod and autopod. A similar phase-in of axial polarity control has been proposed for dorsal–ventral limb axis determination. Analysis of tissue-manipulation experiments, cell-lineage tracing in the chick, and of *lmx1b*-null mice has led to the proposal that stylopod dorsal–ventral limb polarity is determined before the limb bud forms. Subsequently, during the limb bud stages, the ectoderm controls zeugopod and autopod dorsal–ventral polarity through *Wnt7a* expression (reviewed in Chen and Johnson, 1999). Nelson *et al.* (1996) also proposed that the stylopod is a *Shh*-independent segment of the limb. Interestingly, these authors show a correlation in the expression of *Shh* and the differential and unique Hox paralogue gene expressions in chick zeugopod and autopod. This supports the notion of a context-dependent response of each limb segment to the *Shh* signal (Nelson *et al.*, 1996).

The data from the $Shh^{-/-}$ mutant make it apparent that *Shh* is not necessary for the limb bud to emerge from the lateral plate. Similarly, *Shh* expression is not detectable in the limb buds of the *limbless* chick mutant. However,

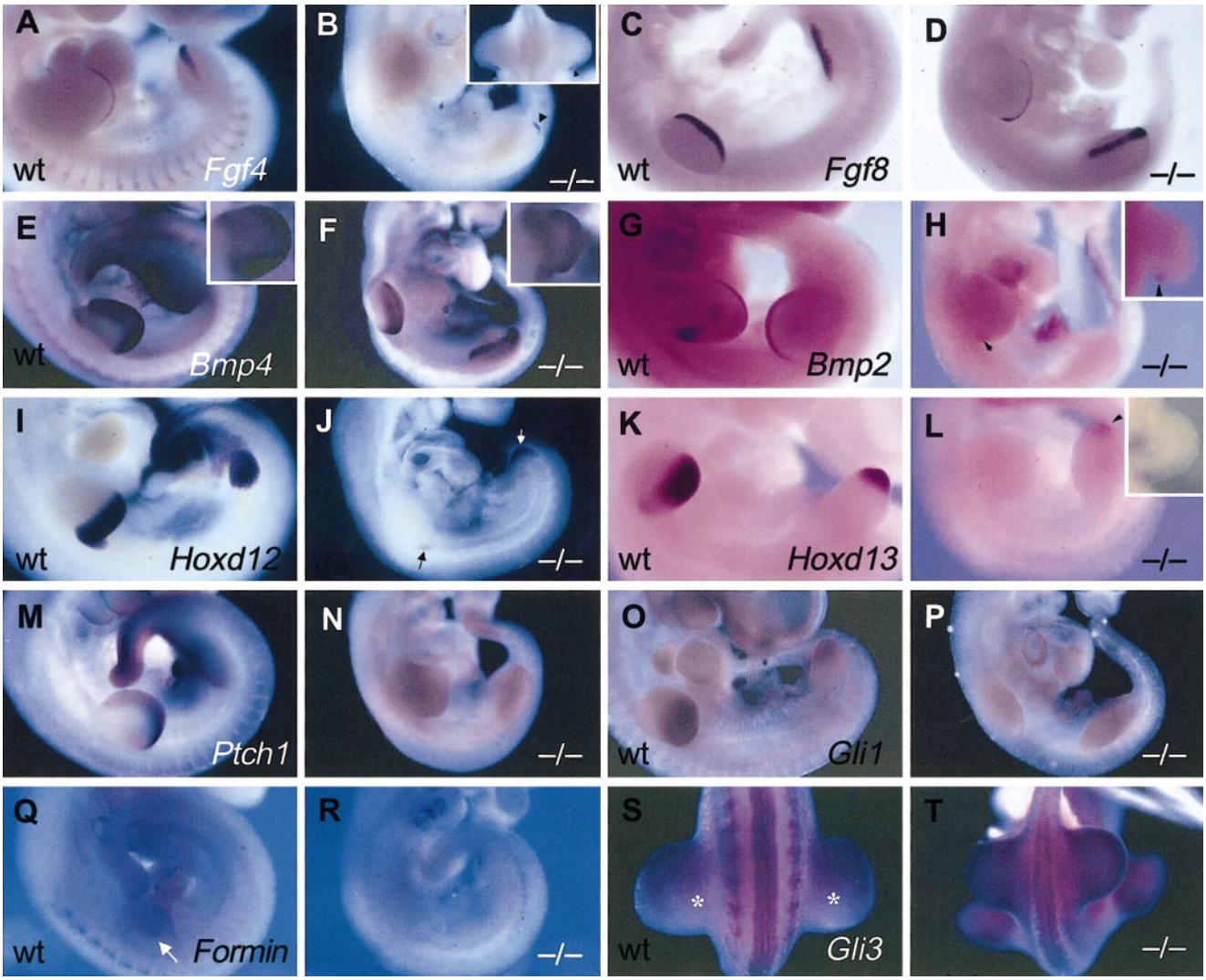

FIG. 6. AER and mesoderm gene expression in *Shh*$^{-/-}$ limbs. Whole-mount *in situ* hybridization of 10.5-dpc wild-type (A, C, E, G, I, K, M, O, Q, S) and *Shh*$^{-/-}$ (B, D, F, H, J, L, N, P, R, T) limbs with probe against *Fgf4* (A, B), *Fgf8* (C, D), *Bmp4* (E, F), *Bmp2* (G, H), *Hoxd12* (I, J), *Hoxd13* (K, L), *Ptch1* (M, N), *Gli1* (O, P), *Formin* (Q, R), and *Gli3* (S, T). Note the arrowhead in (B) marks *Fgf4* expression in the *Shh*$^{-/-}$ AER. The arrow in (H) and (J) indicates the polarized expression of *Bmp2* and *Hoxd12*, respectively, in the *Shh*$^{-/-}$ limbs. The arrow in (Q) is to indicate the normal Formin expression in the wild-type forelimb. In (S), the asterisk marks the posterior mesoderm devoid of *Gli3* expression in the hindlimb. The insets in (B) and (L) represent a higher magnification of the hindlimbs, while the insets in (E), (F), and (H) are of the forelimbs.

limbless does not form an AER (no *Fgf4* or *-8* expression) and is a bidorsal bud without a dorsal–ventral interface (Grieshammer *et al.*, 1996; Noramly *et al.*, 1996; Ros *et al.*, 1996b). The lack of an AER results in complete elimination of the *limbless* limb buds by cell death after initial budding (Carrington and Fallon, 1988). This is a clear indication that the asymmetrically patterned *limbless* limb bud is unstable. If a wild-type AER (Carrington and Fallon, 1988) or exogenous FGFs (Grieshammer *et al.*, 1996; Noramly *et al.*, 1996; Ros *et al.*, 1996a) are supplied to the *limbless* bud, the *limbless* mesoderm is stabilized, *Shh* is expressed and a normal limb skeleton develops. In both *Shh*$^{-/-}$ and *limbless* mutants, there are anterior–posterior asymmetries of gene expression in the emergent limb. In addition, the postaxial limb bud border in the *limbless* mutant has the competence to express *Shh* when supplied with FGF; this is also a molecular and functional asymmetry of the emergent limb bud mesoderm. The observations on *limbless* chick and *Shh*$^{-/-}$ mouse point to the conclusion that initial axial organization and emergence of the limb bud are indepen-

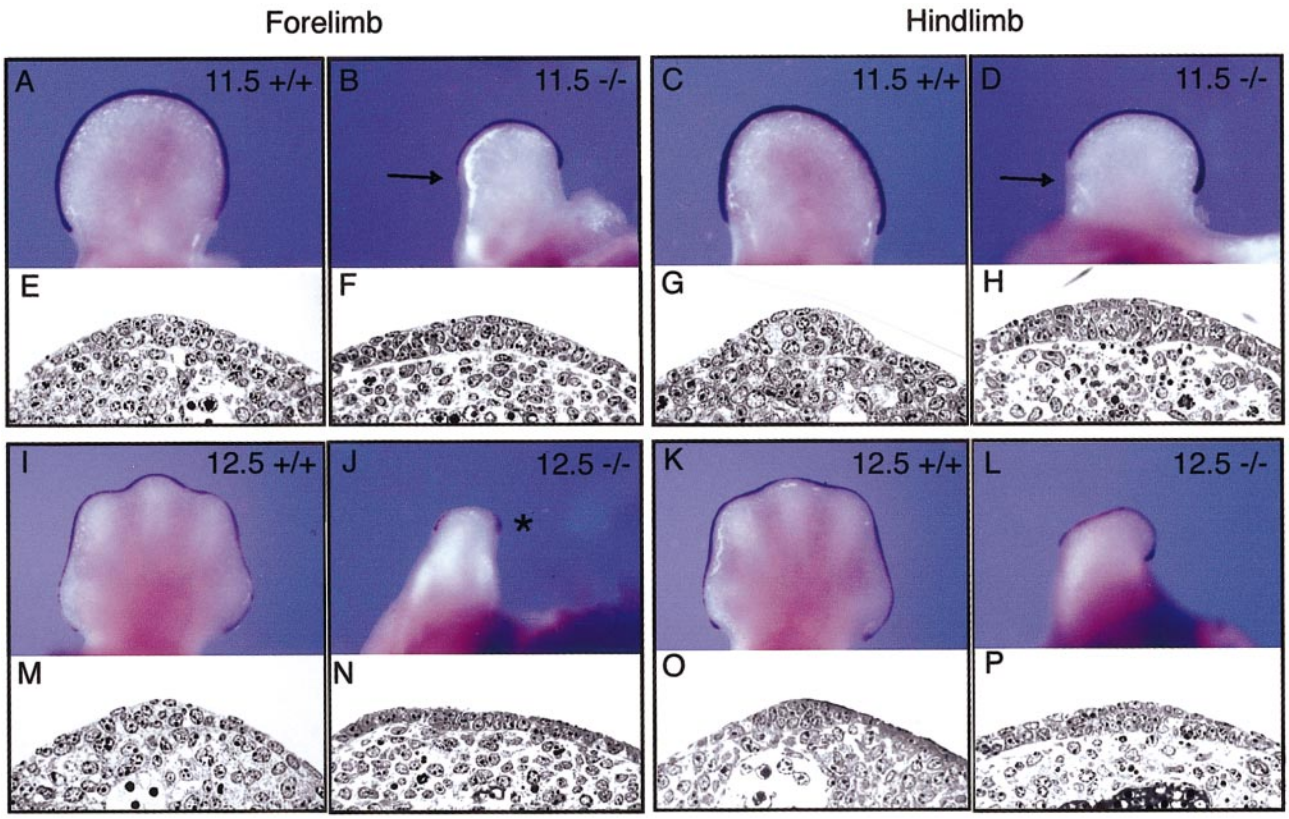

FIG. 7. *Fgf8* expression and structure of the AER. *Fgf8* whole-mount *in situ* hybridization of 11.5- and 12.5-dpc wild-type (A, C, I, K) and $Shh^{-/-}$ (B, D, J, L) limb buds. Whole-mount hybridization specimens are compared to histological cross sections of AERs from comparably staged wild-type (E, G, M, O) and $Shh^{-/-}$ (F, H, N, P) mouse limbs. The approximate location of section is the middle of each bud. Forelimb (11.5 dpc: A, B, E, F; 12.5 dpc: I, J, M, N) and hindlimb (11.5 dpc: C, D, G, H; 12.5 dpc: K, L, O, P) are compared. Arrows in (B) and (D) indicate anterior regions where *Fgf8* is not detected in the mutant compared to the wild-type sibling limbs. The asterisk in (J) marks posterior *Fgf8* expression that maintains a tall ridge morphology.

dent of the three signaling centers that are the hallmark of later limb development.

The conditions and the molecular mechanisms that determine the specifications of the limb-field prepattern are a major question for future studies; clearly, cues from the central body axis must play some role in the determination of the limb field (Coates and Cohn, 1998; Cohn *et al.*, 1997). The hypothesis has been proposed that the expression of the Hox9 paralogous group of transcription factors is a critical component in this process. Cohn *et al.* (1997) show that prospective limb-field territories are marked within the lateral plate mesoderm by overlapping expression of Hox9 paralogues. This proposal is supported by experiments in which *Hox9* expression patterns are altered when supernumerary limbs are induced in the flank by grafting beads loaded with FGFs (Cohn *et al.*, 1995; Ohuchi *et al.*, 1995). Recently, Kawakami *et al.* (2001) reported that *Wnt-2b* and *Wnt-8c* are expressed in mesoderm medial to the chick wing and leg limb fields, respectively, and control *Fgf10* expression in the emerging limb fields. Relating this information to how the particular limb specification events proposed here are achieved, i.e., the prepattern, is not presently apparent.

A recent study on the role of *Shh* in zebrafish pectoral fin development provides interesting confirmation and contrast to the data reported here. *Shh* is expressed along the posterior border of the zebrafish pectoral fin bud with associated expression of genes such as *Ptch1* and *-2*, *BMP2* (Akimenko and Ekker, 1995; Neumann *et al.*, 1999), and *5′* Hoxd and Hoxa paralogues (Sordino *et al.*, 1995). These are similar to patterns for tetrapod limb bud mesoderm as is the expression of *BMP2* and *Fgf8* in the AER analog of the fin bud called the apical ectodermal fold (Neumann *et al.*, 1999). The latter authors have shown the *sonic you* mutant zebrafish, which lacks fin bud *Shh* expression, has transient anterior–posterior fin bud polarity in that *Hoxd11* and *-12* and *Hoxa11* and *-12* are asymmetrically expressed, but the *Hox13* genes are not expressed. These data show some similarity to our observations in the $Shh^{-/-}$ mouse limb. However, in the *sonic you* mutant fin bud, the apical

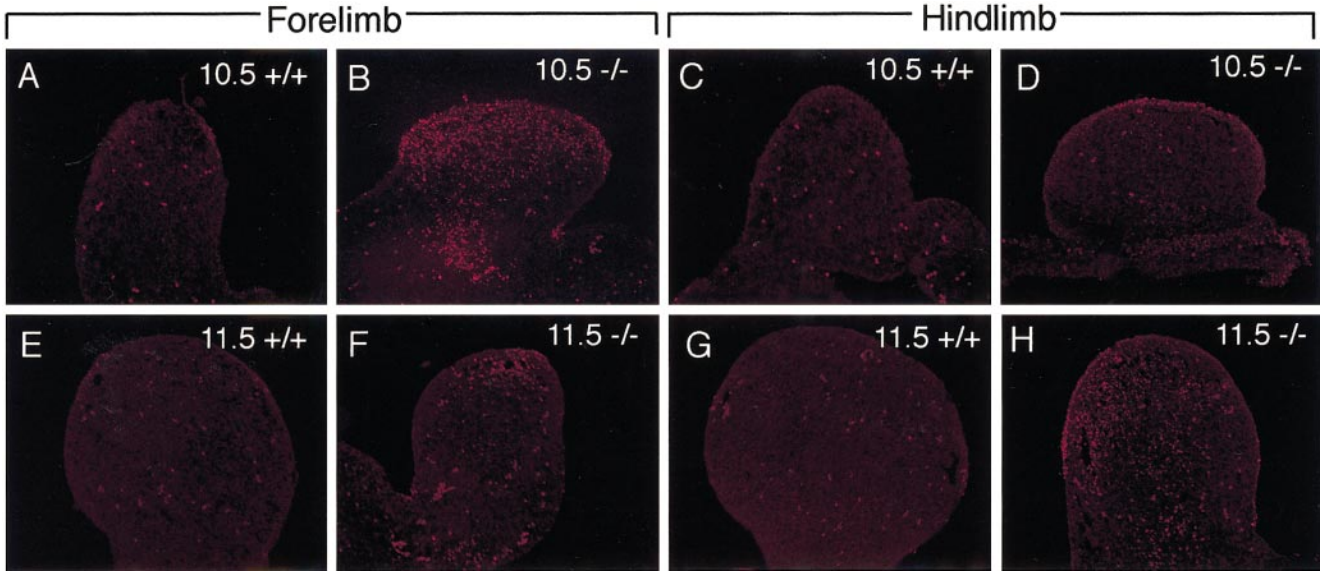

FIG. 8. TUNEL analysis of mutant limbs. Patterns of cell death, shown by TUNEL in 10.5- (A–D) and 11.5-dpc (E–H) *Shh*$^{-/-}$ and wild-type limbs. In each panel, the anterior mesoderm is on the left side. TUNEL staining (compare A, E, C, G with B, F, D, H, respectively) indicated an increase in cell death in the anterior mesoderm of mutant fore- and hindlimb when compared to wild-type limbs. Control sections for false-positive signals due to autoflourescence were performed and background signals were negligible (data not shown).

ectodermal fold fails to form, resulting in the absence of endoskeleton formation of the pectoral fin (Neumann *et al.*, 1999). In contrast, we have shown that, although its structure eventually is compromised, mouse AER formation is independent of *Shh* expression and its maintenance in the *Shh*$^{-/-}$ mutant permits the stabilization of limb skeletal elements. However, in the absence of *Shh*, expansion of the distal anterior–posterior axis of the limb bud fails to occur.

In summary, we propose that the ZPA, through the actions of *Shh*, in conjunction with the AER expands the limb-field prepattern along the limb bud anterior–posterior axis; *Shh* function becomes necessary at or just distal to the prospective elbow and knee joints. There is now a significant body of data that demonstrates the emerging limb bud is a triaxially polarized structure that requires an FGF or FGFs to become a stable entity. While the three-limb bud-organizing centers normally begin expression very early, even before bud emergence, they are not necessary for the initial triaxial limb bud organization. Moreover, several lines of evidence indicate that the stylopod is completely specified in the limb field. Because there is also competence to form recognizable but imperfect zeugopod and autopod elements without *Shh* input, the role of *Shh* in stimulating cell proliferation and survival of limb bud mesoderm assumes critical importance. It will be of great interest to dissect the integration of *Shh*, *Wnts*, *Fgf*s, and the *Hox* genes in permitting the realization of zeugopod and autopod development. This will lead to an understanding of how the competence to form initial zeugopod and autopod skeletal elements, determined in the limb field, is expanded to give these segments complete anterior–posterior polarity and identity.

ACKNOWLEDGMENTS

This work was initially conducted in collaboration with Dr. Heiner Westphal, whom we would like to thank for his encouragement. We thank Y. Sun and Y.-F. Wang for mouse husbandry, Dr. Edward Bersu for helpful discussion on developmental anatomy, and Diana Myers for preparing the manuscript. We also thank C. Hui, G. Martin, S. Lee, D. Duboule, M. Scott, A. McMahon, A. Joyner, B. Hogan, and P. Leder for the cDNA probes. This work is supported by NIH Grant 37489 (to C.C.), a Basil O'Connor Award (to C.C.), and NIH Grant 32551 (to J.F.F.). M.P.H. was supported in part by NIH TG32 HD07477 and a Cremer Fellowship from the University of Wisconsin Medical School. P.A.B. is an investigator of the Howard Hughes Medical Institute. We thank S&R Egg Farm (Whitewater, WI) for providing the White leghorn flock.

REFERENCES

Ahlgren, S. C., and Bronner-Fraser, M. (1999). Inhibition of sonic hedgehog signaling in vivo results in craniofacial neural crest cell death. *Curr. Biol.* **9,** 1304–1314.

Akimenko, M., and Ekker, M. (1995). Anterior duplication of the *Sonic hedgehog* expression pattern in the pectoral fin buds of zebrafish treated with retinoic acid. *Dev. Biol.* **170,** 243–247.

Bell, S. M., Schreiner, C. M., and Scott, W. J. (1999). Disrupting the establishment of polarizing activity by teratogen exposure. *Mech. Dev.* **88,** 147–157.

Borycki, A.-G., Brunk, B., Tajbakhsh, S., Buckingham, M., Chiang, C., and Emerson, C. P. (1999). Sonic hedgehog controls epaxial muscle determination through Myf5 activation. *Development* **126,** 4053–4063.

Carrington, J. L., and Fallon, J. F. (1988). Initial limb budding is independent of apical ectodermal ridge activity: Evidence from a limbless mutant. *Development* **104,** 361–367.

Charité, J., McFadden, D. G., and Olson, E. N. (2000). The bHLH transcription factor dHAND controls *Sonic hedgehog* expression and establishment of the zone of polarizing activity during limb development. *Development* **127,** 2461–2470.

Chen, H., and Johnson, R. L. (1999). Dorsoventral patterning of the vertebrate limb: A process governed by multiple events. *Cell Tissue Res.* **296,** 67–73.

Chiang, C., Litingtung, Y., Lee, E., Young, K. E., Corden, J. L., Westphal, H., and Beachy, P. A. (1996). Cyclopia and defective axial patterning in mice lacking *Sonic hedgehog* gene function. *Nature* **383,** 407–413.

Chiang, C., Swan, R., Grachtchouk, M., Bolinger, M., Litingtung, Y., Robertson, E., Cooper, M., Gaffield, W., Westphal, H., Beachy, P., and Dlugosz, A. (1999). Essential role for Sonic hedgehog during hair follicle morphogenesis. *Dev. Biol.* **205,** 1–9.

Coates, M. I., and Cohn, M. J. (1998). Fins, limbs and tails: Outgrowth and patterning in vertebrate evolution. *BioEssays* **20,** 371–381.

Cohn, M. J., Izpisua-Belmonte, J. C., Abud, H., Heath, J. K., and Tickle, C. (1995). Fibroblast growth factors induce additional limb development from the flank of chick embryos. *Cell* **80,** 739–746.

Cohn, M. J., Patel, K., Krumlauf, R., Wilkinson, D. G., Clarke, J. D., and Tickle, C. (1997). *Hox9* genes and vertebrate limb specification. *Nature* **387,** 97–101.

Fallon, J. F., and Crosby, G. M. (1975). Normal development of the chick wing following removal of the polarizing zone. *J. Exp. Zool.* **193,** 449–455.

Fallon, J. F., and Kelley, R. O. (1977). Ultrastructural analysis of the apical ectodermal ridge during vertebrate limb morphogenesis. II. Gap junctions as distinctive ridge structures common to birds and mammals. *J. Embryol. Exp. Morphol.* **41,** 223–232.

Fernandez-Teran, M., Piedra, M. E., Kathiriya, I. S., Srivastava, D., Rodriguez-Rey, J. C., and Ros, M. A. (2000). Role of dHAND in the anterior-posterior polarization of the limb bud: Implications for the Sonic hedgehog pathway. *Development* **127,** 2133–2142.

Grieshammer, U., Minowada, G., Pisenti, J. M., Abbott, U. K., and Martin, G. R. (1996). The chick *limbless* mutation causes abnormalities in limb bud dorsal- ventral patterning: implications for the mechanism of apical ridge formation. *Development* **122,** 3851–3861.

Hamburger, V., and Hamilton, H. L. (1951). A series of normal stages in the development of the chick embryo. *J. Morphol.* **88,** 49–92.

Hayes, C., Brown, J. M., Lyon, M. F., and Morriss-Kay, G. M. (1998). *Sonic hedgehog* is not required for polarising activity in the *Doublefoot* mutant mouse limb bud. *Development* **125,** 351–357.

Henrique, D., Adam, J., Myat, A., Chitnis, A., Lewis, J., and Ish-Horowicz, D. (1995). Expression of a Delta homologue in prospective neurons in the chick. *Nature* **375,** 787–790.

Johnson, R. L., and Tabin, C. J. (1997). Molecular models for vertebrate limb development. *Cell* **90,** 979–990.

Kawakami, Y., Capdevila, J., Büscher, D., Itoh, T., Rodríguez Esteban, C., and Izpisua Belmonte, J. C. (2001). WNT signals control FGF-dependent limb initiation and AER induction in the chick embryo. *Cell* **104,** 891–900.

Kochhar, D. M. (1973). Limb development in mouse embryo. I. Analysis of teratogenic effects of retinoic acid. *Teratology* **7,** 289–298.

Kraus, P., Fraidenraich, D., and Loomis, C. A. (2001). Some distal limb structures develop in mice lacking Sonic hedgehog signaling. *Mech. Dev.* **100,** 45–58.

Lewandoski, M., Sun, X., and Martin, G. R. (2000). Fgf8 signalling from the AER is essential for normal limb development. *Nat. Genet.* **26,** 460–463.

Litingtung, Y., Lei, L., Westphal, H., and Chiang, C. (1998). Sonic hedgehog is essential to foregut development. *Nat. Genet.* **20,** 58–61.

Lopez-Martinez, A., Chang, D. T., Chiang, C., Porter, J. A., Ros, M. A., Simandl, B. K., Beachy, P. A., and Fallon, J. F. (1995). Limb-patterning activity and restricted posterior localization of the amino-terminal product of Sonic hedgehog cleavage. *Curr. Biol.* **5,** 791–796.

Martin, G. R. (1998). The roles of FGFs in the early development of vertebrate limbs. *Genes Dev.* **12,** 1571–1586.

Moon, A. M., Boulet, A. M., and Capecchi, M. R. (2000). Normal limb development in conditional mutants of *Fgf4*. *Development* **127,** 989–996.

Moon, A. M., and Capecchi, M. R. (2000). Fgf8 is required for outgrowth and patterning of the limbs. *Nat. Genet.* **26,** 455–459.

Nelson, C. E., Morgan, B. A., Burke, A. C., Laufer, E., DiMambro, E., Murtaugh, L. C., Gonzales, E., Tessarollo, L., Parada, L. F., and Tabin, C. (1996). Analysis of *Hox* gene expression in the chick limb bud. *Development* **122,** 1449–1466.

Neumann, C. J., Grandel, H., Gaffield, W., Schulte-Merker, S., and Nüsslein-Volhard, C. (1999). Transient establishment of anteroposterior polarity in the zebrafish pectoral fin bud in the absence of *sonic hedgehog* activity. *Development* **126,** 4817–4826.

Ng, J. K., Tamura, K., Büscher, D., and Izpisua Belmonte, J. C. (1999). Molecular and cellular basis of pattern formation during vertebrate limb development. *Curr. Top. Dev. Biol.* **41,** 37–66.

Noramly, S., Pisenti, J., Abbott, U., and Morgan, B. (1996). Gene expression in the limbless mutant: Polarized gene expression in the absence of Shh and an AER. *Dev. Biol.* **179,** 339–346.

Ohuchi, H., Nakagawa, T., Yamauchi, M., Ohata, T., Yoshioka, H., Kuwana, T., Mima, T., Mikawa, T., Nohno, T., and Noji, S. (1995). An additional limb can be induced from the flank of the chick embryo by FGF4. *Biochem. Biophys. Res. Commun.* **209,** 809–816.

Pagan, S. M., Ros, M. A., Tabin, C., and Fallon, J. F. (1996). Surgical removal of limb bud *Sonic hedgehog* results in posterior skeletal defects. *Dev. Biol.* **180,** 35–40.

Pearse, R. V., and Tabin, C. J. (1998). The molecular ZPA. *J. Exp. Zool.* **282,** 677–690.

Reginelli, A. D., Wang, Y.-Q., Sassoon, D., and Muneoka, K. (1995). Digit tip regeneration correlates with regions of *Msx1 (Hox 7)* expression in fetal and newborn mice. *Development* **121,** 1065–1076.

Ros, M. A., Lopez-Martinez, A., Simandl, B. K., Rodriguez, C., Izpisua Belmonte, J. C., Dahn, R., and Fallon, J. F. (1996a). The limb field mesoderm determines initial limb bud anteroposterior asymmetry and budding independent of sonic hedgehog or apical ectodermal gene expressions. *Development* **122,** 2319–2330.

Ros, M. A., Lopez-Martinez, A., Simandl, B. K., Rodriguez, C., Izpisua-Belmonte, J. C., Dahn, R., and Fallon, J. F. (1996b). Insights into gene expression associated with limb budding using

a limbless mutant. In "5th International Limb Development and Regeneration Conference," York, U.K.

Ros, M. A., Simandl, B. K., Clark, A. W., and Fallon, J. F. (2000). Methods for manipulating the chick limb bud to study gene expressions, tissue interactions and patterning. In "Development Biology Protocols" (R. S. Tuan and C. W. Lo, Eds.), pp 245–266. Humana Press, Clifton, NJ.

Rubin, L., and Saunders, J. J. (1972). Ectodermal-mesodermal interactions in the growth of limb buds in the chick embryo: Constancy and temporal limits of the ectodermal induction. *Dev. Biol.* **28,** 94–112.

Sanz-Ezquerro, J. J., and Tickle, C. (2000). Autoregulation of *Shh* expression and Shh induction of cell death suggest a mechanism for modulating polarising activity during chick limb development. *Development* **127,** 4811–4823.

Schaller, S. A., Li, S., Ngo-Muller, V., Han, M. J., Omi, M., Anderson, R., and Muneoka, K. (2001). Cell biology of limb patterning. *Int. Rev. Cytol.* **203,** 483–517.

Shubin, N., Tabin, C., and Carroll, S. (1997). Fossils, genes and the evolution of animal limbs. *Nature* **388,** 639–648.

Sordino, P., van der Hoeven, F., and Duboule, D. (1995). Hox gene expression on teleost fins and the origin of vertebrate digits. *Nature* **375,** 678–681.

St-Jacques, B., Dassule, H. R., Karavanova, I., Botchkarev, V. A., Li, J., Danielian, P., McMahon, J. A., Lewis, P. M., Paus, R., and McMahon, A. P. (1998). Sonic hedgehog signaling is essential for hair development. *Curr. Biol.* **8,** 1058–1068.

Stocum, D. L. (1995). "Wound Repair, Regeneration and Artificial Tissues." R. G. Landes, Austin.

Storm, E. E., and Kingsley, D. M. (1996). Joint patterning defects caused by single and double mutations in members of the bone morphogenetic protein (BMP) family. *Development* **122,** 3969–3979.

Stratford, T., Horton, C., and Maden, M. (1996). Retinoic acid is required for the initiation of outgrowth in the chick limb bud. *Curr. Biol.* **6,** 1124–1133.

Sun, X., Lewandoski, M., Meyers, E. N., Liu, Y. H., Maxson, R. E., and Martin, G. R. (2000). Conditional inactivation of Fgf4 reveals complexity of signalling during limb bud development. *Nat. Genet.* **25,** 83–86.

Tanaka, M., Cohn, M. J., Ashby, P., Davey, M., Martin, P., and Tickle, C. (2000). Distribution of polarizing activity and potential for limb formation in mouse and chick embryos and possible relationships to polydactyly. *Development* **127,** 40011–40021.

Todt, W. L., and Fallon, J. F. (1987). Posterior apical ectodermal ridge removal in the chick wing bud triggers a series of events resulting in defective anterior pattern formation. *Development* **101,** 501–515.

Wang, B., Fallon, J. F., and Beachy, P. A. (2000). Hedgehog-regulated processing of Gli3 produces an anterior/posterior repressor gradient in the developing vertebrate limb. *Cell* **100,** 423–434.

Yang, Y., Drossopoulou, G., Chuang, P.-T., Duprez, D., Marti, E., Bumcrot, D., Vargesson, N., Clarke, J., Niswander, L., McMahon, A., and Tickle, C. (1997). Relationship between dose, distance and time in *Sonic Hedgehog*-mediated regulation of anteroposterior polarity in the chick limb. *Development* **124,** 4393–4404.

Yang, Y., Guillot, P., Boyd, Y., Lyon, M. F., and McMahon, A. P. (1998). Evidence that preaxial polydactyly in the *Doublefoot* mutant is due to ectopic Indian Hedgehog signaling. *Development* **125,** 3123–3132.

Zákány, J., and Duboule, D. (1999). *Hox* genes in digit development and evolution. *Cell Tissue Res.* **296,** 19–25.

Zákány, J., Fromental-Ramin, C., Warot, X., and Duboule, D. (1997). Regulation of number and size of digits by posterior Hox genes: A dose-dependent mechanisms with potential evolutionary implications. *Proc. Natl. Acad. Sci. USA* **94,** 13695–13700.

Zeller, R., and Duboule, D. (1997). Dorso-ventral limb polarity and origin of the ridge: On the fringe of independence? *BioEssays* **19,** 541–546.

Zúñiga, A., Haramis, A.-P. G., McMahon, A., and Zeller, R. (1999). Signal relay by BMP antagonism controls the SHH/FGF4 feedback loop in vertebrate limb buds. *Nature* **401,** 598–602.

Zwilling, E. (1955). Ectoderm-mesoderm relationship in the development of the chick embryo limb bud. *J. Exp. Zool.* **128,** 423–442.

Zwilling, E. (1964). Development of fragmented and dissociated limb bud mesoderm. *Dev. Biol.* **9,** 20–37.

Received for publication October 16, 2000
Revised June 4, 2001
Accepted June 4, 2001
Published online July 10, 2001